NEOPLASMA accepted, ahead of print manuscript
Cite article as https://doi.org/10.4149/neo_2021_210609N773

Running title: Phycocyanin inhibits pancreatic cancer metastasis

Phycocyanin inhibits pancreatic cancer metastasis via suppressing epithelial- mesenchymal transition and targeting Akt/β-catenin pathway

Rongrong Huang#, Gaoyong Liao#, Meifeng Gao, Yu Ou*

School of Life Science and Technology, China Pharmaceutical University, Nanjing, China

*Correspondence: ouyu2008@126.com

#Contributed equally to this work.

Received June 9, 2021 / Accepted July 13, 2021

According to our previous research, phycocyanin (PC) could inhibit pancreatic tumor growth obviously. However, little is known about the effects of phycocyanin on pancreatic tumor metastasis. This study was aimed to investigate whether phycocyanin inhibits pancreatic cancer cells' metastasis and the potential underlying mechanisms. Human pancreatic carcinoma cell lines PANC-1 and BxPC3 were treated with phycocyanin (5, 10, 20, and 40 μM) for 48 h or 72 h. BALB/c nude mice were inoculated intravenously with luciferase-PANC-1 cells to establish a tumor metastasis model. BALB/c nude mice were also inoculated subcutaneously with PANC-1 cells to establish a xenograft tumor model. Our results indicated that (1) phycocyanin inhibited migration, invasion, and movement of pancreatic cancer cells in vitro, and tumor metastasis in mouse xenograft tumor model; (2) phycocyanin significantly changed cell morphology and epithelial-mesenchymal transition (EMT) phenotype in pancreatic cancer cells; (3) phycocyanin decreased the phosphorylation level of Akt and the level of nuclear β-catenin. Moreover, administration of Akt activator SC79 counteracted the inhibitory effect of phycocyanin on the migration of pancreatic cancer cells, associated with the reversal of epithelial-mesenchymal transition and Akt/β-catenin signaling pathway. Taken together, our results suggest that phycocyanin inhibits pancreatic cancer metastasis via suppressing epithelial-mesenchymal transition and targeting the Akt/β-catenin pathway.

Key words: phycocyanin; pancreatic cancer cells; metastasis; epithelial-mesenchymal transition (EMT); Akt/β-catenin

Pancreatic adenocarcinoma (PDAC) is a common malignant digestive system tumor in the world, which is highly aggressive. Although great strides are being made in medical science, the five-year survival rate for pancreatic cancer is still lower than 9% [1, 2]. Among various factors leading to cancer death, tumor metastasis has always been considered an important one [3]. Therefore,

treatment of pancreatic cancer also faces the challenge of tumor metastasis. Epithelial-mesenchymal transition (EMT) is of vital importance to tumor metastasis in the early stage [4] and essential to the epithelium-originated solid tumor metastasis cascade [5, 6]. In EMT process, the connection between cells becomes loose, while the epithelial cells still remain intact, followed with decreasing of cell polarity. Cells begin to show the characteristics of interstitial cells, eventually leading to increased cell invasiveness [3, 7]. Meanwhile, cell morphological and migration behavior turn similar to fibrosis along with epithelial marker E-cadherin downregulated and interstitial marker upregulated. The decreased expression of E-cadherin is the most common indicator of the initiation of EMT, and is related to the development of tumor metastasis [8]. Hence, EMT has represented a novel and major target in anticancer therapy [9]. It is generally known that secondary tumor metastasis is caused by tumor cell adhesion, migration, and proteolysis of extracellular matrix (ECM). MMPs are vital factors to promote tumor metastasis by selectively regulating tumor microenvironment, and it is also an inducer of EMT [10]. Among MMPs family, MMP9 can degrade almost all the components of ECM, and regulate most signal pathways that promote EMT [11, 12]. Cell adhesion molecules also play vital roles in EMT process. Intercellular adhesion molecule-1 (ICAM-1) and vascular adhesion molecule-1 (VCAM-1) were reported to be upregulated as part of the mesenchymal phenotype during EMT, and participated in the dissociation and migration of cancer cells [13, 14]. Thus, these factors can also be used as EMT markers in EMT related researches.

Akt is a pivotal serine/threonine kinase in biological progress including cell proliferation, apoptosis, and metabolism, and is known to promote EMT in tumor metastasis [15]. Available researches have confirmed that Akt pathway plays an important role in EMT process and tumor metastasis of pancreatic cancer. In addition, Akt participates in the modulation of EMT- specific proteins including E- cadherin and vimentin [16, 17]. As all known, β-catenin stabilization is essential for tumor invasion and metastasis in various cancer cells [18]. Evidence has shown that Akt can directly or indirectly act on β-catenin, leading to its stabilization, increasing its transcriptional activity, and promoting EMT [19].

The cyanobacterium *Spirulina platensis*, known as spirulina, contains a lot of bioactive compounds [20]. Phycocyanin (PC), one of the major biliproteins present in spirulina, exerts multiple physiological effects, and has a potential value in the area of functional and healthy food [21]. Our

75 previous study has indicated that phycocyanin can act as an anti-pancreatic cancer agent due to its
76 ability to induce pancreatic cancer cells apoptosis and autophagy [22]. In this study, we approach to
77 investigate whether and how phycocyanin inhibits the invasion and metastasis of pancreatic cancer
78 cells. Our findings suggest that phycocyanin has an Akt/β-catenin-dependent mechanism in
79 EMT-mediated migration and invasion of pancreatic cancer cells.
80

81 **Materials and methods**

82 **Reagents**. Phycocyanin was isolated and purified from *Spirulina platensis* according to the
83 protocols reported previously [23]. Isolated phycocyanin was prepared as a stock solution of 1 mM
84 in PBS (pH 7.4) and stored at -80 °C. Before each experiment, the phycocyanin stock solution was
85 diluted with RPMI-1640 medium (Gibco, USA). Nucleoprotein Extraction Kit was obtained from
86 Beyotime Biotechnology (China). Primary antibody to E-cadherin (#3195), vimentin (#5741),
87 fibronectin (#26836) and keratin (#13063) were available from Cell Signaling Technology (USA).
88 Primary antibody against ICAM-1 (sc-8439), VCAM-1 (sc-13160), MMP-9 (sc-393859) and
89 β-catenin (sc-7963) were purchased from Santa Cruz Biotechnology (USA). Primary antibody
90 against α-tubulin (#AF5001) and GAPDH (#AF1186) were available from Beyotime Biotechnology
91 (China). Secondary antibody HRP-conjugated Goat Anti-Rabbit IgG (#D110058) and
92 HRP-conjugated Goat anti-mouse IgG (#D110087) were available from Sangon Biotech (China).
93 D-luciferin (#2591-17-5) was from Sigma (Germany). SC79 (SML0749) was obtained from
94 Sigma-Aldrich (USA).

95 **Cell culture.** Human pancreatic carcinoma cell lines PANC-1 and BxPC3 purchased from ATCC
96 were cultured in RPMI-1640 at 37 °C in humidified air containing 5% CO_2. The culture medium
97 was supplemented with 10% FBS, penicillin G (100 U/ml) and streptomycin (100 mg/ml).

98 **Cell morphology assay.** PANC-1 and BxPC3 cells were cultured in 12-well plates for 12 h in a
99 density of 6×10^4/well, then phycocyanin (5, 10, 20 and 40 μM) were added to the medium. The
100 cell morphology of each well was recorded with a microscope (Zeiss Series 120) 48 h later.

101 **Microtubule morphology assay.** PANC-1 and BxPC3 cells were seeded into 96-well plates,
102 containing 1×10^4 cells each well. High concentration of phycocyanin group (40 μM) were used to
103 treat each kind of cells respectively for 48 h the next day, and then fixed with 4% paraformaldehyde
104 in PBS for 1 h at room temperature. Afterwards, cells were permeabilized with 0.5% Triton X 100

105 for 10 min, blocked for 30 min with 2% BSA-PBS and incubated for 1 h with the
106 Rabbit-anti-α-tubulin antibody (dilution 1:200) in PBS at room temperature. They were then
107 incubated with the secondary antibody (dilution 1:500) for 1 h at room temperature. DAPI (dilution
108 1:2000) staining was then carried out during 5 min at room temperature after secondary antibody
109 incubation. The fluorescence of each cell was photographed on the High Content Screening
110 Instrument (Molecule Devices [ImageXpress]), and the image was fitted by merge with the software
111 of the instrument. The mean fluorescence intensity of α-tubulin was measured by ImageJ (Version
112 1.48).

113 **Wound healing assay.** To determine cell migration, PANC-1 and BxPC3 cells were seeded at 1 ×
114 10^5 cells per well in 12-well plates. When cells were confluent, a pipette tip was used to scratch cell
115 monolayer across the diameter of each well. The new serum-free medium was added after removing
116 former medium and dislodged cells. The cells were incubated at 37 °C for 1 h, and then the medium
117 was replaced by the medium with phycocyanin (5, 10, 20 and 40 μM) dissolved in 1%
118 FBS-Medium. Cells that migrated to the scratch area were photographed at 0 h and 72 h time points.
119 The cell-free area was measured by ImageJ (Version 1.48). The value of migration area was the
120 difference between the cell-free area at 0 h and the cell-free area at 72 h.

121 **Cell invasion assay.** Matrigel invasion assay was performed to examine the invasion ability of
122 PANC-1 and BxPC3 cells. Briefly, the upper surface of the membrane was coated with Matrigel.
123 Cancer cells were suspended in FBS-free medium, and then seeded in the upper chamber.
124 Phycocyanin was added to a final concentration of 5, 10 and 20 μM. The bottom chamber of the
125 transwell plate was filled with culture medium containing 10% FBS, and the cells migrated to the
126 bottom surface of the transwell chambers through pores 48 h later. Then, they were fixed with
127 formaldehyde and stained with 0.1% Crystal Violet. Under the Olympus inverted microscope, each
128 group was counted with four randomly selected microscopic fields.

129 **Cell mobility assay.** PANC-1 cells were maintained in 96-well plates for 24 h, then labeled with
130 Qtracker565 Cell Labeling Kit (ThermoFisher) according to the instructions. Phycocyanin
131 maintained in RPMI-1640 medium supplemented with 1% FBS was then added into each well at
132 the series concentrations of 5, 10 and 20 μM. Images were captured with a dynamic observation
133 every 30 min for 48 h, and the location of the cells was recorded by the High Content Screening
134 Instrument (Molecule Devices [ImageXpress]).

135 **Construction of Luciferase-PANC-1 stable cell line.** PANC-1 cells were seeded into 96-well
136 plates at a concentration of 1×10^5 cell/well, then different concentrations of puromycin were added
137 to corresponding holes to select an appropriate concentration. Luciferase plasmid virus packaging
138 was taken according to manufacturer's protocol (Guangzhou FulenGen Co., Ltd.). The supernatant
139 was collected to detect virus titer 48 h later strictly following the product instructions. Collected
140 virus was diluted into three concentration gradients. After 24 h infection, the cells were pressed by
141 Puromycin. After five days of pressure screening, the cell growth of the normal group and the
142 infection group was compared. When the difference was found, the monoclonal to the 96-well plate
143 was selected by the finite dilution method, and the use of puromycin was gradually reduced. Several
144 monoclonal were picked out to expand culture and freeze. The activated clones were frozen and
145 preserved for at least one week after the identification. The repetitive luciferase functional
146 identification of seven clones after the passage of the recovered cells was carried out. The luciferase
147 activity was identified strictly according to the luciferase activity detection kit (Promega)
148 instructions. D-luciferin was used to confirm that each clone was successfully labelled with
149 luciferase gene (Supplementary Figure S1).
150 **Tumor metastasis model and Luciferase imaging.** The animal procedures were performed in
151 accordance with the guidelines of the institutional animal care and use committee of China
152 Pharmaceutical University Licensing Committee (License No. SYXK (SU) 2018-0019). The
153 experiment was conducted according to approved guidelines. Six-week-old BALB/c nude mice
154 were inoculated intravenously with Luciferase-PANC-1 stable cell lines (1×10^6 cells in 200 μl of
155 serum-free RPMI-1640 medium). Two days after inoculation, phycocyanin was injected
156 intraperitoneally every two days to mice of different group at the concentrations of 12.5 mg/kg, 25
157 mg/kg and 50 mg/kg respectively during a thirty-day experiment. At the end of the experiment,
158 mice were anesthetized by isoflurane, and then were injected intraperitoneally with D-luciferin
159 substrate (150 mg/kg in PBS) 10 min before imaging. Light emission from luciferase was detected
160 by using a living animal imaging system (NightOwl LB983, Berthold Technologies).
161 **Xenograft tumor experiment.** The animal procedures were performed in accordance with the
162 guidelines of the institutional animal care and use committee of China Pharmaceutical University
163 Licensing Committee (License No. SYXK (SU) 2018-0019). The experiment was conducted
164 according to approved guidelines. Six-week-old BALB/c nude mice were inoculated

165 subcutaneously with human pancreatic carcinoma PANC-1 cells (5 × 10^6 cells in 100 μl of
166 serum-free RPMI-1640 medium) into the axillary fossa. The mice were randomly divided into four
167 groups with three mice for each group. They are 0.9% normal saline group (control), 10 mg/kg
168 phycocyanin group, 25 mg/kg phycocyanin group and 50 mg/kg phycocyanin group. During the
169 thirty-day experiment, phycocyanin and vehicle were injected intraperitoneally to mice every two
170 days. At the end of treatment, all mice were sacrificed and tumors were excised for further
171 immunohistochemistry assay and western blot assay.

172 **Immunohistochemistry assay.** The tissue was embedded by paraffin and then cut into 3-μm thick
173 continuous sections by using a microtome (Finesse ME, Thermo Scientific). The slides went
174 through the following steps including drying and dewaxing by xylene, rehydration by graded
175 ethanol, blocking endogenous peroxidase activity by immersion in 3% hydrogen peroxide for 10
176 min and antigen recovery by autoclaving for 3 min in citrate buffer (pH=6). In order to avoid
177 nonspecific reaction, the slides were incubated with 5% BSA for 15 min before incubation with the
178 indicated primary antibody (dilution 1:200) for 50 min at 37 °C and subsequently incubation with a
179 secondary antibody (dilution 1:1000) for 30 min at 37 °C. Then they were stained with DAB
180 (3,3-diaminobenzidine) and counterstained with Mayer's hematoxylin. The last steps were
181 dehydration and mounting. In the negative control, a normal rabbit IgG replaced the primary
182 antibody.

183 **Western blot assay.** Tumor tissues and cells were washed with ice-cold PBS. Their lysates were
184 obtained by incubation for 20 min in buffer of 50 mM Tris-HCl (pH 7.4), 150 mM NaCl, 1 mM
185 EDTA, 1 mg/ml pepstatin A, 1 mM PMSF and 1% Triton X-100. The homogenate was centrifuged
186 for 20 min with 10,000 × g, and then the supernatant was collected and quantified by BCA
187 (Bicinchoninic acid). The nucleoproteins were obtained with a Nucleoprotein Extraction Kit. The
188 lysates were loaded to 10-14% SDS-PAGE and transferred to PVDF membranes. Then the
189 membranes underwent sequentially the blocking, the incubation with the primary antibodies
190 (dilution 1:1000) at 4 °C for 12 h and the incubation with secondary antibodies (dilution 1:5000)
191 conjugated with corresponding horseradish peroxidase for 1 h. After each incubation step,
192 membranes were washed in Tris-buffered saline containing 0.5% Tween-20 for 3 times, each time
193 for 5 min. ECL was used to visualize the corresponding bands with Tanon-5200 Chemiluminescent
194 Imaging System (Tanon Science & Technology Co.,Ltd).

195 **Statistical analysis.** Data were expressed as the mean±SD. The statistical significance of the
196 differences between the experimental variables and their reference group was determined using the
197 Student's *t*-test; $p < 0.05$ was considered statistically significant.
198
199 **Results**
200 **Phycocyanin inhibits migration, invasion and movement of pancreatic cancer cells *in vitro*.**
201 Cell migration experiment showed that phycocyanin (5, 10, 20 and 40 μM) inhibited PANC-1 and
202 BxPC3 cells migration in a dose dependent manner (Figures 1A, 1B). Phycocyanin also inhibited
203 cell invasion ability significantly (Figure 1C). The number of invasion cells gradually decreased
204 from 200 to about 10 by treating with phycocyanin (Figure 1D). Referring to the effects of
205 phycocyanin on PANC-1 cell movement, the result of real-time scanning imaging assay suggested
206 that the trajectory (Figure 1E position) and the movement range (Figure 1E distance) of almost all
207 normal cells were longer, while the number of long trajectory cells decreased dose-dependently
208 with the treatment of phycocyanin. The results fully demonstrated that phycocyanin inhibited the
209 movement of pancreatic cancer cells.
210 **Phycocyanin changed cell morphology and EMT markers in pancreatic cancer cells.** During
211 EMT, the distribution and expression of cytoskeleton altered, usually companied by the change of
212 cell morphology [15]. As shown in Figure 2A, under the treatment of phycocyanin (5, 10, 20 and 40
213 μM), PANC-1 and BxPC3 cells showed obvious morphological alteration. Immunofluorescence
214 assay further confirmed that phycocyanin altered the morphology and distribution of microtubules
215 significantly (Figures 2B, 2C). Furthermore, phycocyanin also increased the expression of epithelial
216 cell marker molecules E-Cadherin and keratin-8 in pancreatic cancer cell lines time-dependently,
217 while reduced the expression of interstitial cell marker molecules N-cadherin, fibronectin and
218 vimentin (Figure 2D).
219 **Phycocyanin inhibited the metastasis of pancreatic cancer cells *in vivo*.** To investigate the
220 inhibitory effect of phycocyanin on the tumor metastasis, PANC-1-Luciferase cells were used to
221 track the movement of tumor cells in nude mice. As shown in Figure 3A, PANC-1-Luciferase cells
222 in control group transferred throughout the body along with intense luminescence, while under the
223 treatment of phycocyanin, tumor metastasis was obviously suppressed dose-dependently, especially
224 in the high dose group. In order to verify the inhibition of phycocyanin on EMT, we firstly detected

225 ICAM-1, VCAM-1 and MMP-9 expression in xenograft tumor in the nude mice. As shown in
226 Figure 3B, phycocyanin could reduce the expression of ICAM-1, VCAM-1 and MMP-9 in tumor
227 tissues. For further confirmation, we used immunohistochemistry assay to detect the expression
228 level of epithelial marker E-cadherin and interstitial markers vimentin and fibronectin in tumor
229 tissues. As shown in Figures 3C and 3D, phycocyanin could significantly increase the expression
230 level of E-cadherin and decrease expression levels of vimentin and fibronectin. Combined the
231 results of the expression of EMT markers *in vitro* and *in vivo*, phycocyanin significantly changed
232 EMT phenotype in pancreatic cancer cells.

233 **Phycocyanin inhibited the Akt/β-catenin pathway in pancreatic cancer cells.** To determine the
234 downstream mechanisms underlying the role of phycocyanin in the metastasis of pancreatic cancer
235 cells, phycocyanin was examined in terms of inhibiting Akt activity. As expected, introduction of 20
236 μM phycocyanin into PANC-1 and BxPC3 cells significantly suppressed Akt phosphorylation
237 (Figure 4A). These results indicated that phycocyanin normally acted to suppress Akt activity in
238 pancreatic cancer cells. The transcription factor β-catenin, as a direct or indirect downstream target
239 of Akt, is widely known to crucially affect tumor invasion and metastasis [19]. Hence, the
240 expression of nuclear β-catenin was detected by using western blot assay. As our results shown,
241 phycocyanin reduced nuclear β-catenin level of PANC-1 and BxPC3 cells significantly (Figure 4B).

242 **Akt activator counteracted the inhibitory effect of phycocyanin on the migration of pancreatic**
243 **cancer cells.** To further confirm the relationship between Akt overactivation and the inhibitory
244 effect of phycocyanin on the migration, PANC-1 cells were treated with Akt activator SC79. From
245 the result, SC79 could effectively counteract the inhibitory effect of phycocyanin on Akt
246 phosphorylation in pancreatic cancer cells (Figure 5A). Besides, SC79 also reversed the inhibitory
247 effect of phycocyanin on the migration of PANC-1 and BxPC3 cells (Figures 5B, 5C). Therefore,
248 these results suggested that phycocyanin inhibited the migration of pancreatic cancer cells via pAkt
249 downregulation.

250 **Akt/β-catenin pathway was vital for phycocyanin to suppress pancreatic cancer cell EMT.** Akt
251 activation is known to promote EMT [15]. As shown in Figure 6A, under the action of Akt activator
252 SC79, the phycocyanin-induced expression of EMT biomarkers (E-cadherin, keratin-8, N-cadherin,
253 fibronectin and vimentin) in pancreatic cancer cells was reversed. This result indicated that
254 phycocyanin reversed EMT process through Akt inactivation in pancreatic cancer cells. On the

255 other hand, immunofluorescence assay showed that without SC79, phycocyanin inhibited the
256 nuclear translocation of transcription factor β-catenin, while with SC79, the inhibitory effect was
257 reversed (Figure 6B). Based on these results, Akt/β-catenin axis was thought to potentially mediate
258 the effect of phycocyanin on EMT process of pancreatic cancer cells.
259

260 **Discussion**

261 Increasing evidence showed that phycocyanin has the anti-cancer effect [24]. Our previous study
262 has demonstrated that phycocyanin can inhibit the growth of various cancer cell lines as well as
263 pancreatic cancer effectively in mouse xenograft tumor model [24]. In this study, we used classical
264 cell scratch method and Matrigel matrix gel invasion method to determine the effect of phycocyanin
265 on the metastasis function of pancreatic cancer cells. Additionally, we used real-time live cell
266 imaging to intuitively describe the cell movement of pancreatic cancer cells. Our findings presented
267 that phycocyanin inhibited migration, invasion and movement of pancreatic cancer cells *in vitro*,
268 and the tumor metastasis in mouse xenograft tumor model.
269 The EMT phenotype is associated with pancreatic cancer cell metastasis [25-27]. In fact, there are
270 many natural plant ingredients that can inhibit epithelial mesenchymal transition and show effective
271 anti-cancer effect, mainly including flavonoids, polyphenols and alkaloids [28]. We demonstrated
272 that phycocyanin treatment could suppress EMT phenotype acquisition by down-regulating the
273 mesenchymal cell marker and up-regulating of the epithelial cell marker. The EMT process is a
274 gradual process in highly metastatic tumor and plays a cumulative role in the adhesion of tumor
275 cells at a specific level [3]. Adhesion molecules ICAM-1 and VCAM-1 in tumor tissues play
276 important roles in tumor progression and metastasis [13, 29]. Consequently, it is of great
277 significance to detect the expression of adhesion molecules as a way to measure tumor metastasis
278 [30]. Moreover, matrix metalloproteinases (MMPs) are essential to promote tumor metastasis via
279 selectively regulating the tumor microenvironment to promote tumor cell metastasis, as well as to
280 induce EMT [10]. Activated MMPs degrade ECM components, causing cancer cells expansion
281 without resistance, and there is a positive correlativity between MMP-9 and pancreatic cancer cell
282 invasion [31]. Indeed, our results showed that phycocyanin could significantly reduce the
283 expression of ICAM-1, VCAM-1 and MMP-9 in tumor tissues. These indicated that phycocyanin
284 contributed to inhibiting pancreatic cells metastasis, partly by regulating adhesion molecules and

MMP expression and controlling ECM degradation.

In addition, EMT involves reorganization of the cytoskeleton. During EMT, cell morphology may undergo external changes as a result of changes in the distribution and expression of cytoskeleton [32]. Microtubules are the main components of cytoskeleton, which consist of α and β-tubulin dimers. Through their dynamic characteristics, they have been proved to control the intracellular transport, molecular signaling and directional movement of cells [15]. We used immunofluorescence method to qualitatively analyze the microtubule (α-tubulin) induced by phycocyanin in pancreatic cancer cells, and the results showed that the distribution of microtubules in pancreatic cancer cells was altered by phycocyanin.

Akt activation could promote EMT [15], and impact on cancer cells growth, polarity, migration and invasion [18]. It has been reported that EMT regulation need the involvement of β-catenin in multiple human cancers [33]. Enhancement of β-catenin stability and transcriptional activity caused by Wnt-dependent or independent signal transduction plays a key role in tumor invasion and metastasis [18]. Activated Akt can stabilize β-catenin by phosphorylation and/or inhibiting GSK-3β, thereby removing it from cell-to-cell contacts and nuclear accumulation [19]. In the present study, we found that phycocyanin blocked the activation of Akt and the nuclear localization of β-catenin in pancreatic cancer cells. To validate the role of Akt/β-catenin pathway, we used the Akt activator SC79 to maintain Akt activation in pancreatic cancer cells. The results showed that the effect of phycocyanin on pancreatic cancer cell migration and EMT phenotype was completely suppressed by Akt activator SC79. In addition, the decreased level of nuclear β-catenin in the pancreatic cancer cells when treated with phycocyanin was also increased when SC79 used. It is possible to indicate that Akt/β-catenin pathway is involved in the role of phycocyanin against pancreatic cancer metastasis.

Taken together, our results reveal the function and mechanisms of phycocyanin in regulating pancreatic tumor metastasis. We demonstrated that phycocyanin inhibited pancreatic cancer cells metastasis via suppressing epithelial- mesenchymal transition and targeting Akt/β-catenin pathway.

Acknowledgements: This work was funded by the Priority Academic Program Development of Jiangsu Higher Education Institutions (PAPD).

Supplementary data are available in the online version of the paper.

References

[1] RYAN DP, HONG TS, BARDEESY N. Pancreatic adenocarcinoma. N Engl J Med 2014; 371: 1039-1049. http://doi.org/10.1056/NEJMra1404198

[2] QUARESMA M, COLEMAN MP, RACHET B. 40-year trends in an index of survival for all cancers combined and survival adjusted for age and sex for each cancer in England and Wales, 1971-2011: a population-based study. Lancet 2015; 385: 1206-1218. http://doi.org/10.1016/S0140-6736(14)61396-9

[3] KOTIYAL S, BHATTACHARYA S. Events of Molecular Changes in Epithelial-Mesenchymal Transition. Crit Rev Eukaryot Gene Expr 2016; 26: 163-171. http://doi.org/10.1615/CritRevEukaryotGeneExpr.2016016307

[4] RHIM AD, MIREK ET, AIELLO NM, MAITRA A, BAILEY JM et al. EMT and dissemination precede pancreatic tumor formation. Cell 2012; 148: 349-361. http://doi.org/10.1016/j.cell.2011.11.025

[5] HU J, LI L, CHEN H, ZHANG G, LIU H et al. MiR-361-3p regulates ERK1/2-induced EMT via DUSP2 mRNA degradation in pancreatic ductal adenocarcinoma. Cell Death Dis 2018; 9: 807. http://doi.org/10.1038/s41419-018-0839-8

[6] MIYATAKE Y, OHTA Y, IKESHITA S, KASAHARA M. Anchorage-dependent multicellular aggregate formation induces a quiescent stem-like intractable phenotype in pancreatic cancer cells. Oncotarget 2018; 9: 29845-29856. http://doi.org/10.18632/oncotarget.25732

[7] HU Y, YU X, XU G, LIU S. Metastasis: an early event in cancer progression. J Cancer Res Clin Oncol 2017; 143: 745-757. http://doi.org/10.1007/s00432-016-2279-0

[8] MATOS ML, LAPYCKYJL, ROSSO M, BESSO MJ, MENCUCCI MV et al. Identification of a Novel Human E-Cadherin Splice Variant and Assessment of Its Effects Upon EMT-Related Events. J Cell Physiol 2017; 232: 1368-1386. http://doi.org/10.1002/jcp.25622

[9] SALEHI B, VARONI EM, SHARIFI-RAD M, RAJABI S, ZUCCA P et al. Epithelial-mesenchymal transition as a target for botanicals in cancer metastasis. Phytomedicine 2019; 55: 125-136. http://doi.org/10.1016/j.phymed.2018.07.001

[10] CHEN Y, HUANG L, WANG S, LI JL, LI M et al. WFDC2 contributes to epithelial-mesenchymal transition (EMT) by activating AKT signaling pathway and regulating MMP-2 expression. Cancer Manag Res 2019; 11: 2415-2424. http://doi.org/10.2147/CMAR.S192950

[11] SUN SJ, WANG N, SUN ZW, CHEN J, CUI HW. MiR-5692a promotes the invasion and metastasis of hepatocellular carcinoma via MMP9. Eur Rev Med Pharmacol Sci 2018; 22: 4869-4878. http://doi.org/10.26355/eurrev_201808_15623

[12] XU W, YANG Z, LU N. A new role for the PI3K/Akt signaling pathway in the epithelial-mesenchymal transition. Cell Adh Migr 2015; 9: 317-324. http://doi.org/10.1080/19336918.2015.1016686

[13] BAI J, ADRIANI G, DANG TM, TU TY, PENNY HX et al. Contact-dependent carcinoma aggregate dispersion by M2a macrophages via ICAM-1 and beta2 integrin interactions. Oncotarget 2015; 6: 25295-25307. http://doi.org/10.18632/oncotarget.4716

[14] SAMATOV TR, TONEVITSKY AG, SCHUMACHER U. Epithelial-mesenchymal transition: focus on metastatic cascade, alternative splicing, non-coding RNAs and modulating compounds. Mol Cancer 2013; 12: 107. http://doi.org/10.1186/1476-4598-12-107

[15] PONGRAKHANANON V, WATTANATHAMSAN O, TAKEICHI M, CHETPRAYOON P, CHANVORACHOTE P. Loss of CAMSAP3 promotes EMT via the modification of microtubule-Akt machinery. J Cell Sci 2018; 131: jcs216168. http://doi.org/10.1242/jcs.216168

[16] LIAO G, WANG M, OU Y, ZHAO Y. IGF-1-induced epithelial-mesenchymal transition in MCF-7 cells is mediated by MUC1. Cell Signal 2014; 26: 2131-2137. http://doi.org/10.1016/j.cellsig.2014.06.004

[17] LI W, JIANG Z, XIAO X, WANG Z, WU Z et al. Curcumin inhibits superoxide dismutase-induced epithelial-to-mesenchymal transition via the PI3K/Akt/NF-kappaB pathway in pancreatic cancer cells. Int J Oncol 2018; 52: 1593-1602. http://doi.org/10.3892/ijo.2018.4295

[18] WANG C, RUAN P, ZHAO Y, LI X, WANG J et al. Spermidine/spermine N1-acetyltransferase regulates cell growth and metastasis via AKT/beta-catenin signaling pathways in hepatocellular and colorectal carcinoma cells. Oncotarget 2017; 8: 1092-1109. http://doi.org/10.18632/oncotarget.13582

[19] FANG D, HAWKE D, ZHENG Y, XIA Y, MEISENHELDER J et al. Phosphorylation of beta-catenin by AKT promotes beta-catenin transcriptional activity. J Biol Chem 2007; 282: 11221-11229. http://doi.org/10.1074/jbc.M611871200

[20] CARRIZZO A, CONTE GM, SOMMELLA E, DAMATO A, AMBROSIO M et al. Novel Potent Decameric Peptide of Spirulina platensis Reduces Blood Pressure Levels Through a PI3K/AKT/eNOS-Dependent Mechanism. Hypertension 2019; 73: 449-457. http://doi.org/10.1161/HYPERTENSIONAHA.118.11801

[21] HAO S, LI S, WANG J, ZHAO L, YAN Y et al. C-Phycocyanin Suppresses the In Vitro Proliferation and Migration of Non-Small-Cell Lung Cancer Cells through Reduction of RIPK1/NF-kappaB Activity. Mar Drugs 2019; 17: 362. http://doi.org/10.3390/md17060362

[22] LIAO G, GAO B, GAO Y, YANG X, CHENG X et al. Phycocyanin Inhibits Tumorigenic Potential of Pancreatic Cancer Cells: Role of Apoptosis and Autophagy. Sci Rep 2016; 6: 34564. http://doi.org/10.1038/srep34564

[23] SEO Y C, CHOI W S, PARK JH, PARK JO, JUNG KH et al. Stable isolation of phycocyanin from Spirulina platensis associated with high-pressure extraction process. Int J Mol Sci 2013; 14: 1778-1787. http://doi.org/10.3390/ijms14011778

[24] JIANG L, WANG Y, YIN Q, LIU G, LIU H et al. Phycocyanin: A Potential Drug for Cancer Treatment. J Cancer 2017; 8: 3416-3429. http://doi.org/10.7150/jca.21058

[25] CHEN J, LI Q, AN Y, LV N, XUE X et al. CEACAM6 induces epithelial-mesenchymal transition and mediates invasion and metastasis in pancreatic cancer. Int J Oncol 2013; 43: 877-885. http://doi.org/10.3892/ijo.2013.2015

[26] YEUNG KT, YANG J. Epithelial-mesenchymal transition in tumor metastasis. Mol Oncol 2017; 11: 28-39. http://doi.org/10.1002/1878-0261.12017

402 [27] SINGH M, YELLE N, VENUGOPAL C, SINGH SK. EMT: Mechanisms and therapeutic
403 implications. Pharmacol Ther 2018; 182: 80-94.
404 http://doi.org/10.1016/j.pharmthera.2017.08.009
405 [28] ZHANG L, WANG X, LAI M. Modulation of epithelial-to-mesenchymal cancerous
406 transition by natural products. Fitoterapia 2015; 106: 247-255.
407 http://doi.org/10.1016/j.fitote.2015.09.013
408 [29] ROSETTE C, ROTH RB, OETH P, BRAUN A, KAMMERER S et al. Role of ICAM1 in
409 invasion of human breast cancer cells. Carcinogenesis 2005; 26: 943-950.
410 http://doi.org/10.1093/carcin/bgi070
411 [30] VON BURSTIN J, BACHHUBER F, PAUL M, SCHMID RM, RUSTGI AK. The TALE
412 homeodomain transcription factor MEIS1 activates the pro-metastatic melanoma cell
413 adhesion molecule Mcam to promote migration of pancreatic cancer cells. Mol Carcinog
414 2017; 56: 936-944. http://doi.org/10.1002/mc.22547
415 [31] GRUNWALD B, VANDOOREN J, GERG M, AHOMAA K, HUNGER A et al. Systemic
416 Ablation of MMP-9 Triggers Invasive Growth and Metastasis of Pancreatic Cancer via
417 Deregulation of IL6 Expression in the Bone Marrow. Mol Cancer Res 2016; 14: 1147-1158.
418 http://doi.org/10.1158/1541-7786.MCR-16-0180
419 [32] YILMAZ M, CHRISTOFORI G. EMT, the cytoskeleton, and cancer cell invasion. Cancer
420 Metastasis Rev 2009; 28: 15-33. http://doi.org/10.1007/s10555-008-9169-0
421 [33] WANG X, WANG S, LI X, JIN S, XIONG F et al. The critical role of EGF-beta-catenin
422 signaling in the epithelial-mesenchymal transition in human glioblastoma. Onco Targets
423 Ther 2017; 10: 2781-2789. http://doi.org/10.2147/OTT.S138908
424

425 **Figure Legends**

426

427 **Figure 1.** Phycocyanin inhibited migration, invasion and movement of pancreatic cancer cells *in*
428 *vitro.* A) Wound healing assay was performed to assess the effect of phycocyanin on the migration
429 of PANC-1 and BxPC3 human pancreatic cancer cells. The cells were treated with different doses of
430 phycocyanin for 72 h. The 0 h panel indicates the original space between the cell layers immediate
431 after making a scratch (×200 magnification). Scale bar=100 μm. B) Quantitation of the cells wound
432 healing assay. Data were presented as mean±SD, ***$p < 0.001$ vs. Control, n=3. C) Matrigel
433 invasion assay was performed to examine the effect of phycocyanin on the invasive capacity of
434 PANC-1 and BxPC3 cells. The cells were seeded in Matrigel-coated Boyden chambers and were
435 incubated with different doses of phycocyanin as indicated. After 48 h, the cells invading the
436 membranes were stained and then counted (×200 magnification). Scale bar=100 μm. D)
437 Quantitation of the cell invasion. Data were presented as mean±SD, **$p < 0.01$ vs. Control, n=4. E)
438 Effect of phycocyanin on the pancreatic cancer cell motion. The movement tracks of PANC-1 cells
439 along the time-lapse sequences from the first frame to the 96 th frames, covering 48 h *in vitro*. The

440 tracks have been automatically corrected and verified (position). Mean deviation of cell positions
441 was obtained by the registration software from those obtained using Retrac against the all the 96
442 frames (distance).
443
444 **Figure 2.** Effects of phycocyanin on the morphology, microtubule morphology and the transition
445 from mesenchymal-to-epithelial in pancreatic cancer cells. A) Phycocyanin induced the
446 morphological changes of PANC-1 and BxPC3 cells. Cells were treated with indicated
447 concentration of phycocyanin and images were taken at the indicated time points (×400
448 magnification). Scale bar=50 μm. B) Phycocyanin-induced change of cytoskeletal structure of
449 pancreatic cells. PANC-1 and BxPC3 cells were incubated without (Control) or with 40 μM
450 phycocyanin in serum-containing medium for 48 h. These cells were fluorescence-stained for
451 α-tubulin (green) by using a specific antibody and DAPI (blue). Fluorescence images were obtained
452 with a High Content Screening System (×400 magnification). Scale bar=50 μm. C) Quantitation of
453 the α-tubulin (green) fluorescence intensity. Data were presented as mean±SD, ***$p < 0.001$ vs.
454 Control, n=3. D) The levels of epithelial and mesenchymal biomarkers in PANC-1 and BxPC3 cells
455 after treatment with phycocyanin were verified using western blot analysis.
456
457 **Figure 3.** Phycocyanin inhibited the metastasis of pancreatic cancer cells in nude mice. A) Whole
458 animal imaging analysis of mice (n=3/group). PANC-1-Luciferase cells (1×10^6) were injected
459 intravenously into nude mice (n=3). Mice were treated with intraperitoneal injection of indicated
460 phycocyanin (every other day). Images of mice from control and treatment groups are shown on day
461 30 after cell implantation. B) Western blot analysis for the expression of ICAM-1, VCAM-1 and
462 MMP-9 in tumor tissue (n=3/group). C) Representative images of immunohistochemistry staining
463 of E-cadherin, vimentin and fibronectin in the PANC-1 xenografts (×400 magnification). Scale
464 bar=50 μm. D) Quantitation of the immunohistochemistry staining. Data were presented as
465 mean±SD, ***$p < 0.001$ vs. Control, n=3.
466
467 **Figure 4.** Phycocyanin inhibited the phosphorylation of Akt and β-catenin nuclear translocation in
468 pancreatic cancer cells. A) Western blot analysis of pAkt and total Akt in PANC-1 and BxPC3 cells.
469 GAPDH was shown as a loading control, n=3. B) Western blot analysis of β-catenin in the nucleus.

470 Histone H3 was shown as a loading control, n=3.

471

472 **Figure 5.** Akt activator SC79 counteracts phycocyanin-induced migration inhibition in pancreatic
473 cancer cell line PANC-1. A) p-Akt and Akt were analyzed by immunoblotting. B) Cell migration
474 was examined by wound healing assay. Cells were preincubated with 500 ng/ml SC79 for 1 h and
475 then treated with or without 20 μM phycocyanin for 48 h (×200 magnification). Scale bar=100 μm.
476 C) Quantitation of the cells wound healing assay. Data were presented as mean±SD, ***$p < 0.001$
477 vs. Control, n=3.

478

479 **Figure 6.** Phycocyanin inhibits EMT of pancreatic cancer cells through Akt/β-catenin axis. A) SC79
480 reversed the effect of phycocyanin on EMT. The expression levels of E-cadherin, keratin-8,
481 N-cadherin, fibronectin, and vimentin in PANC-1 and BxPC3 cells were measured by western
482 blotting, n=3. B) The translocation of β-catenin was demonstrated by immunofluorescence staining
483 (×400 magnification). Scale bar=50 μm, n=3.

Fig. 1 Download full resolution image

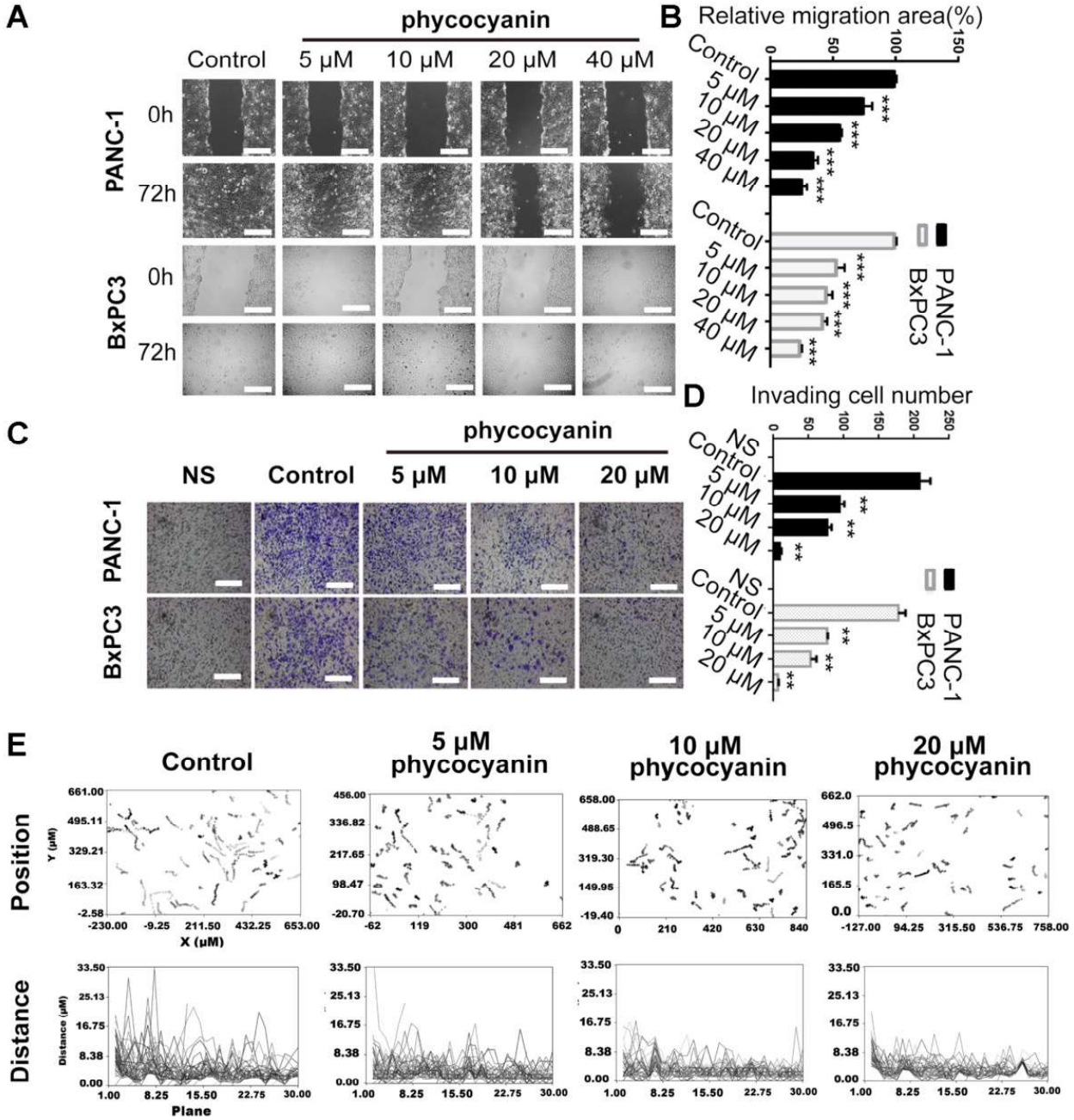

Fig. 2 Download full resolution image

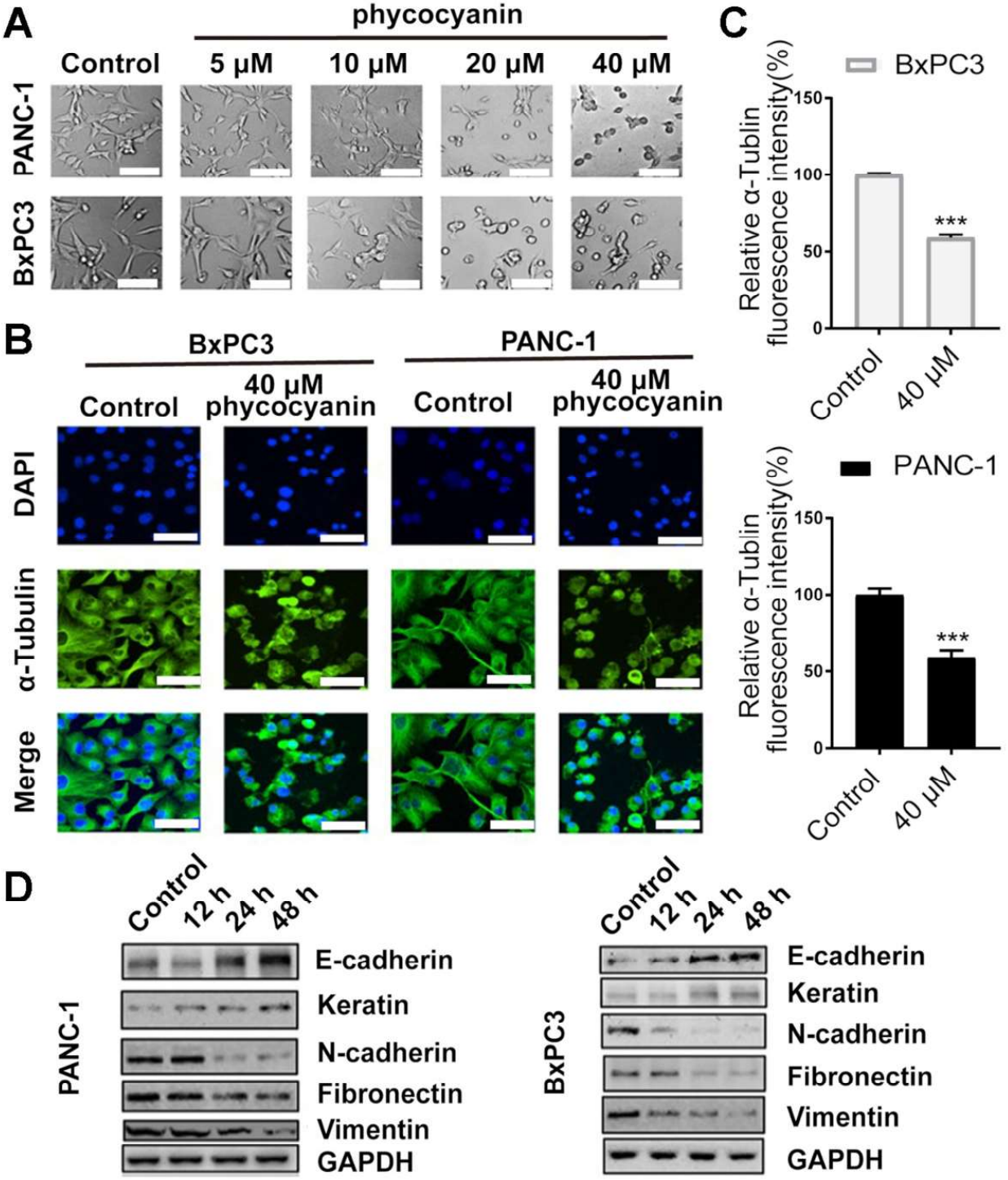

Fig. 3 Download full resolution image

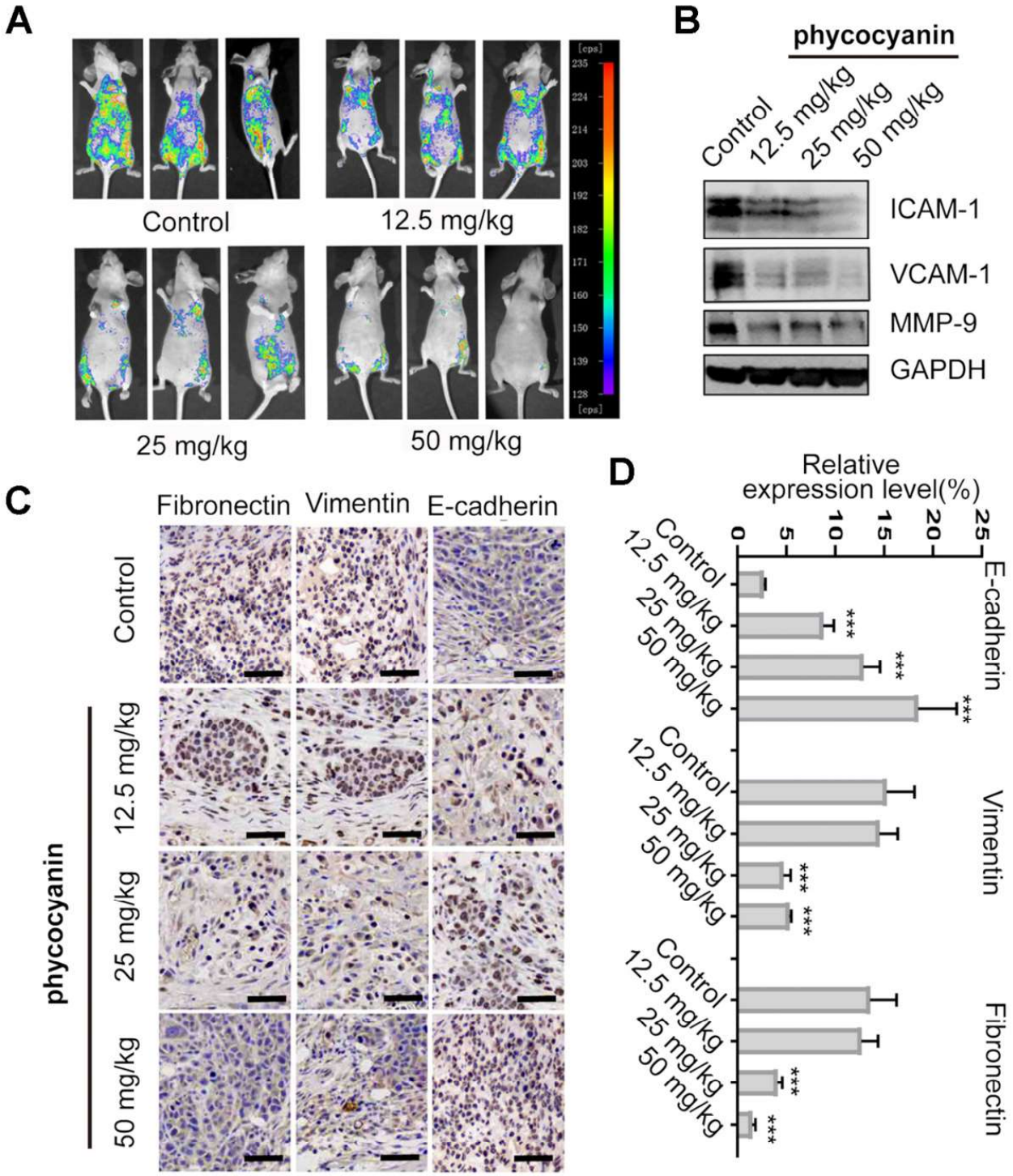

Fig. 4 Download full resolution image

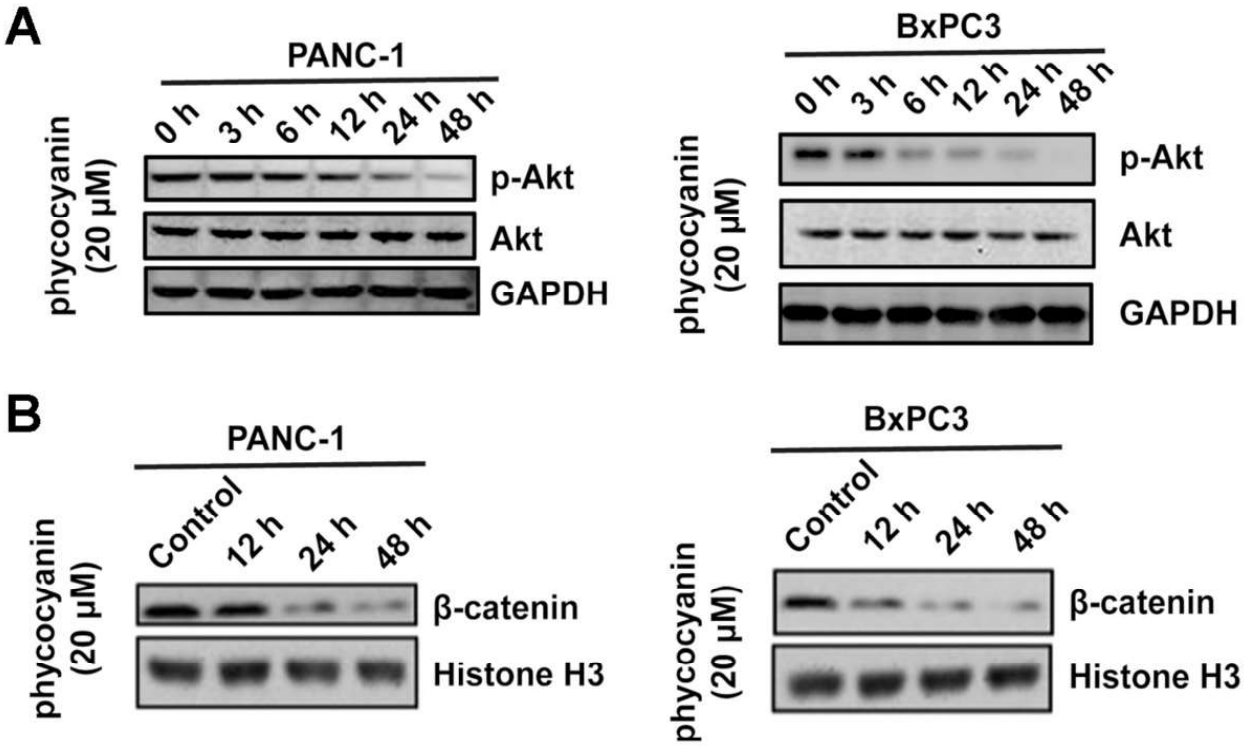

Fig. 5 Download full resolution image

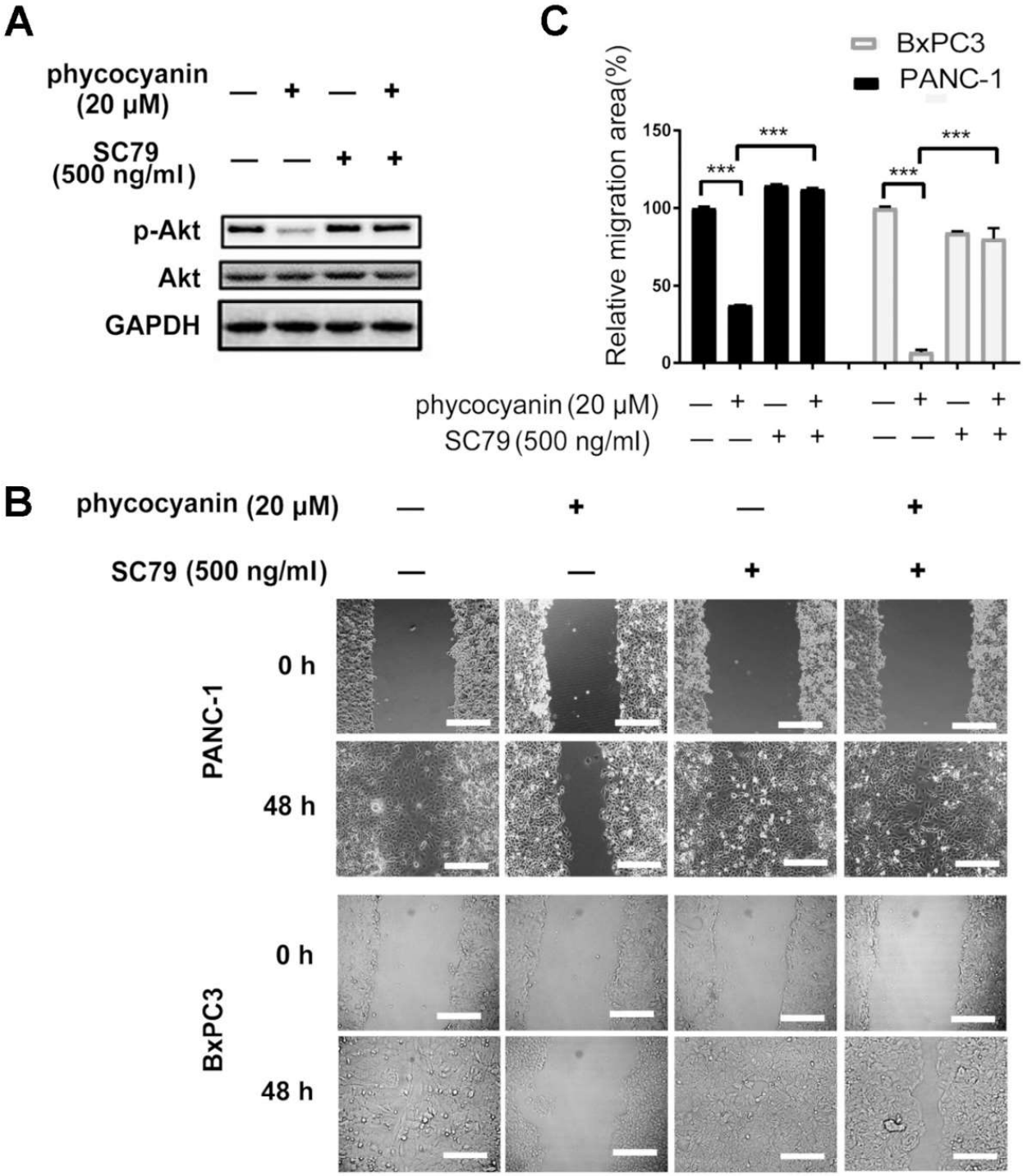

Fig. 6 Download full resolution image